



Swansea University
Prifysgol Abertawe



Cronfa - Swansea University Open Access Repository

This is an author produced version of a paper published in :

Proceedings of the Institution of Mechanical Engineers, Part L: Journal of Materials: Design and Applications

Cronfa URL for this paper:

<http://cronfa.swan.ac.uk/Record/cronfa28394>

Paper:

Hannon, C. & Evans, B. Solid particle erosion protection for the BLOODHOUND SSC front wheel arches. *Proceedings of the Institution of Mechanical Engineers, Part L: Journal of Materials: Design and Applications*

<http://dx.doi.org/10.1177/1464420716659777>

This article is brought to you by Swansea University. Any person downloading material is agreeing to abide by the terms of the repository licence. Authors are personally responsible for adhering to publisher restrictions or conditions. When uploading content they are required to comply with their publisher agreement and the SHERPA RoMEO database to judge whether or not it is copyright safe to add this version of the paper to this repository.

<http://www.swansea.ac.uk/iss/researchsupport/cronfa-support/>

1 Wheel arch CFD analysis

The flow fields in and around the wheel arches were modelled using Flite 3D, a steady state compressible solver capable of modelling supersonic flow conditions (1). The front wheel arch was investigated at two speeds, Mach 1.0 and Mach 1.3 (Figure 1), approximately equivalent to $340 \text{ m}\cdot\text{s}^{-1}$ and $440 \text{ m}\cdot\text{s}^{-1}$ respectively. To reduce computational expense in the CFD modelling of the rotating wheel, a fixed tetrahedral mesh was utilised with no slip boundary conditions applied on solid surfaces corresponding to their relative motions in the moving car reference frame (1). The model assumed no particle entrainment, i.e. a solid ground and air free of particles. The front of the wheel arch only experienced accelerated flow near the forward lip of the arch, which was most likely due to suction from the faster flow outside of the wheel arch. The flow in the rear half of the wheel arch was predicted to be significantly faster at Mach 1.3 than at Mach 1.0, which was caused by a reversal in the flow regime near the rear arch lip, shown by the velocity vectors in Figure 2. The flow velocity in the rear half of the arch at Mach 1.3 ranged from approximately $100 \text{ m}\cdot\text{s}^{-1}$ to $200 \text{ m}\cdot\text{s}^{-1}$. Any particles entrained in the flow would strike the wheel arch at a relatively low impingement angle, indicating a harder material would be more suitable in this region (2). The stagnation point highlighted in Figure 1 and shown in more detail in Figure 2 indicated a tough, rather than hard, material would be best suited at this point, to avoid the intersection of Hertzian cones typical of brittle materials at high impingement angles (2, 3).

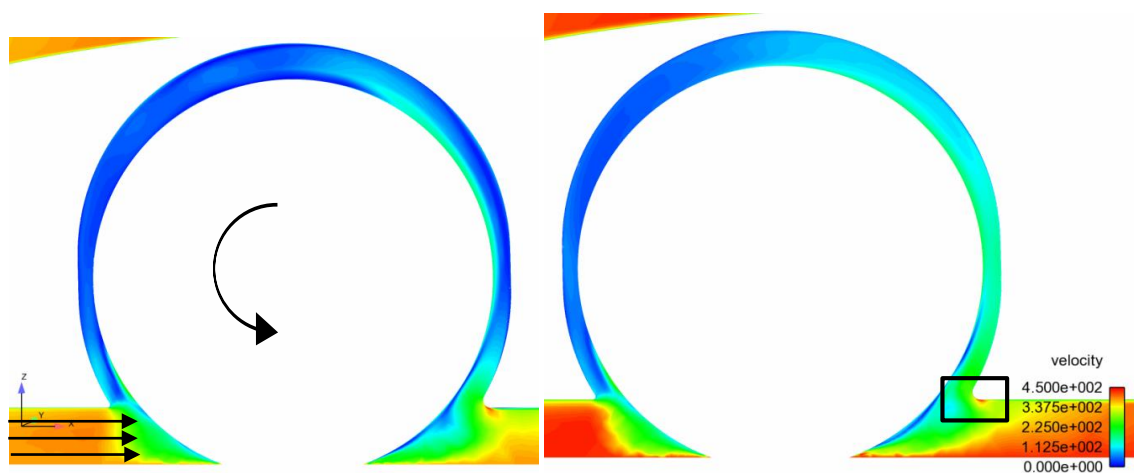


Figure 1: Velocity ($\text{m}\cdot\text{s}^{-1}$) contour plots on the centreline of a front wheel. Mach 1.0 (left) and Mach 1.3 (right). Wheel rotation and upstream velocity vectors are represented using arrows. The region highlighted by a black box is shown in more detail in Figure 2.

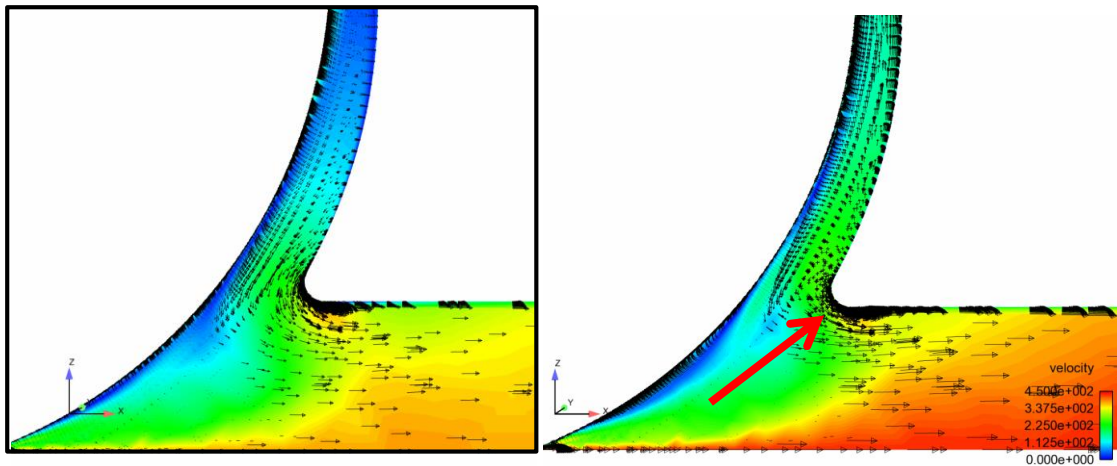


Figure 2: Velocity ($\text{m}\cdot\text{s}^{-1}$) vectors, wheel centreline. Mach 1.0 (Left) and Mach 1.3 (Right). The 90 deg impact angle at the stagnation point is indicated by the red arrow.

1. Evans BJ, Hassan O, Jones JW, Morgan K, Remaki L. Computational Fluid Dynamics Applied to the Aerodynamic Design of a Land-Based Supersonic Vehicle. *Numerical Methods for Partial Differential Equations*. 2011;27:141-59.
2. Hutchings IM. *Tribology: Friction and Wear of Engineering Materials*. UK: Edward Arnold; 1992.
3. Fischer-Cripps AC. Hertzian Fracture. *Introduction to Contact Mechanics*. 2nd ed 2007. p. 115-36.